Re-examining the directional-ordering transition in the compass model with screw-periodic boundary conditions

Sandro Wenzel,[1,2,*] Wolfhard Janke,[3,†] and Andreas M. Läuchli[1,‡]
[1]*Max-Planck-Institute for the Physics of Complex Systems (MPIPKS), Nöthnitzer Str. 38, D-01187 Dresden, Germany*
[2]*Institute of Theoretical Physics, École Polytechnique Fédérale de Lausanne (EPFL), CH-1015 Lausanne, Switzerland*
[3]*Institut für Theoretische Physik and Centre for Theoretical Sciences (NTZ), Universität Leipzig, Postfach 100920, D-04009 Leipzig, Germany*
(Received 19 February 2010; published 9 June 2010)

We study the directional-ordering transition in the two-dimensional classical and quantum compass models on the square lattice by means of Monte Carlo simulations. An improved algorithm is presented which builds on the Wolff cluster algorithm in one-dimensional subspaces of the configuration space. This improvement allows us to study classical systems up to $L=512$. Based on this algorithm, we give evidence for the presence of strongly anomalous scaling for periodic boundary conditions which is much worse than anticipated before. We propose and study alternative boundary conditions for the compass model which do not make use of extended configuration spaces and show that they completely remove the problem with finite-size scaling. In the last part, we apply these boundary conditions to the quantum problem and present a considerably improved estimate for the critical temperature which should be of interest for future studies on the compass model. Our investigation identifies a strong one-dimensional magnetic ordering tendency with a large correlation length as the cause of the unusual scaling and moreover allows for a precise quantification of the anomalous length scale involved.

DOI: 10.1103/PhysRevE.81.066702 PACS number(s): 02.70.Ss, 05.70.Fh, 75.10.Jm

I. INTRODUCTION

The quantum compass model [1] has recently seen a renaissance in condensed-matter physics, which was to a large part triggered by the observation that it may protect q-bits in a quantum computing setting [2,3]. This observation may be of actual practical relevance as the quantum compass model can be realized by a special connection of Josephson junction arrays, a concept with which first experimental successes could be reported [4]. A concrete realization in terms of real materials has also been proposed recently [5]. Apart from the current interest from the quantum information perspective, the quantum compass model is relevant as an effective description for orbital ordering and was originally proposed in this setting [1]. Due to the diverse interest in the model, recent contributions in the literature have studied many different aspects, ranging primarily from detailed investigations of the ground-state properties [2,6] to a study of the possible low-temperature phases and phase transitions in both the classical and quantum cases [7–9]. Complementary to that, recent studies considered modified variants of the compass model in one-dimensional chains [10–12] or in a magnetic field [13]. In Ref. [14], two of us have proposed and studied a two-dimensional (2D) geometric variant of the compass model. The model is also known to have relevance for other settings such as $p+ip$ superconductors [15,16], the concept of dimensional reduction [17], and was recently shown to be isospectral [18] to Kitaev's toric code [19] in a field.

The 2D compass model (CM) is defined on a square lattice of $N=L\times L$ sites as a (pseudo-) spin model by the Hamiltonian

$$\mathcal{H}_{\mathrm{CM}} = J_x \sum_i S_i^x S_{i+\mathbf{e}_x}^x + J_y \sum_i S_i^y S_{i+\mathbf{e}_y}^y, \tag{1}$$

where S_i^x and S_i^y are components of a two-component spin $\mathbf{S}_i$ at site i. The spin can represent both classical and quantum degrees of freedom. In the latter case, S^x and S^y are represented by the usual Pauli matrices, i.e., $\mathbf{S}=(1/2)(\sigma_x,\sigma_y)$. The classical case is analogous to an ordinary classical XY spin $\mathbf{S}=(S^x,S^y)\in S^1$. The interesting feature of Eq. (1) is its anisotropy in spin *and* lattice space.

For $J_y\neq J_x$, the ground state of Eq. (1) can be described by (weakly) coupled Ising spin chains oriented in the x or y direction depending on $|J_x|>|J_y|$ or $|J_y|>|J_x|$, respectively. The quantum phase transition between these differently oriented ground states was shown to be of first order [20,21]. One interesting feature of that work is that Ref. [21] gives one of the first nontrivial applications of the recently introduced infinite pair-entangled tensor product states (iPEPS) [22] which aim at providing a new numerical approach to 2D interacting quantum systems. Following the same line of research, a quantum phase transition in a generalized CM has also been investigated recently [23] using the related multiscale entangled renormalization ansatz (MERA) [24].

Here, we will focus on the symmetric case $J_x=J_y=-1$ which allows—due to a discrete $x\leftrightarrow y$ symmetry in spin and lattice space [7]—for a thermal phase transition to a directionally ordered low-temperature phase without long-range local magnetic order [7,9]. In Ref. [9], two of us have studied this transition extensively for both the classical and quantum CMs. One of the main results of this contribution is the con-

*sandro.wenzel@epfl.ch
†janke@itp.uni-leipzig.de
‡aml@pks.mpg.de

firmation that the CM suffers from extraordinary finite-size corrections when studied in a simple canonical ensemble on the torus, contradicting the naive assumption that generic periodic boundary conditions are optimal. A solution to alleviate this problem had already been suggested in Ref. [7], where the authors proposed the use of so-called fluctuating boundary conditions (FBCs) (sometimes also referred to as "annealed boundary conditions"). These formally place the CM in a larger configuration space where the partition function is given by

$$Z_{\mathrm{FBC}} = \sum_{\{J_b=\pm 1\}} \int \prod_i d\mathbf{S}_i \exp(-\beta \mathcal{H}_{\mathrm{CM}}) \tag{2}$$

instead of just

$$Z_{\mathrm{PBC}} = \int \prod_i d\mathbf{S}_i \exp(-\beta \mathcal{H}_{\mathrm{CM}}) \tag{3}$$

for the standard canonical ensemble with periodic boundary conditions (PBCs). Here, $\{J_b\}$ denotes the set of boundary bonds on the periodic lattice which are allowed to fluctuate between -1 and $+1$ individually [44]. One assumes that the J_b degrees of freedom become unimportant in the thermodynamic limit. Indeed, it was shown in Refs. [7,9] that FBCs lead to very good finite-size scaling (FSS) properties in the classical case from which we have good evidence that the directional-ordering (DO) transition in the CM is in the 2D Ising universality class.

Our good experience with these FBC is unfortunately of no use for the quantum CM because of the minus-sign problem. Furthermore, simulations of the quantum CM are quite demanding and one may currently not reach large lattice sizes (say $L>64$) with reasonable effort. In result, our current estimate of the critical ordering temperature is not very precise as it rests on the use of nonoptimal boundary conditions on moderate lattice sizes [9]. Yet, given the large interest in the model, we find it valuable to try to improve the accuracy of the critical temperature. A better knowledge of such quantities is necessary in order to tackle more advanced features such as the influence of disorder, etc. [8]. Apart from the motivation to improve the available critical data, there are further unsatisfactory points or open problems regarding the previous results [7,9]. These especially concern the *ad hoc* use of FBC to get precise results at the price of introducing extra degrees of freedom to the model. Why do these boundary conditions work so well and why do we observe a complete failure of the critical Binder parameter on periodic lattices? In this work, we (re)address those questions and present improved results on critical properties of the classical and quantum CM that we obtained with a combination of algorithmic advances and by employing so-called screw-periodic boundary conditions.

The outline of the rest of the paper is as follows. In Sec. II, we start with a revision of our Monte Carlo (MC) approach and present an improved MC algorithm building on the Wolff cluster method. The latter will make possible a much more detailed comparison of FSS properties on periodic vs. fluctuating boundary conditions in Sec. III, going considerably beyond Ref. [9]. We will show that periodic boundary conditions behave even worse than previously anticipated. A solution to this problem is thereafter suggested in form of screw-boundary conditions. These will allow to recover very good scaling properties without making use of an extended configuration space (in form of fluctuating boundary conditions). Moreover, they can be readily employed in quantum Monte Carlo (QMC) simulations which is the topic of Sec. IV, where improved critical data for the quantum CM are presented. We end with a summary and conclusions in Sec. V.

II. OBSERVABLES AND MC APPROACH

In this section, we present the standard approach to simulate the classical CM and describe in detail how we can improve the algorithm by making use of ideas from well-known cluster MC updates. A short discussion of the QMC approach for the quantum version of Eq. (1) is postponed to Sec. IV.

A. Revision of classical MC approach and relevant observables

In the classical case, we have investigated the ensembles specified by Eqs. (2) and (3) using the METROPOLIS algorithm combined with the parallel tempering (PT) scheme [25–27] parallelizing simulations at different temperatures. Technical details of this approach are described in Ref. [9]. During a MC simulation, we measure an order parameter known to describe directional ordering

$$D = \frac{1}{N}|E_x - E_y|, \tag{4}$$

with $E_x = \Sigma_i S_i^x S_{i+\mathbf{e}_x}^x$ and $E_y = \Sigma_i S_i^y S_{i+\mathbf{e}_y}^y$. We concentrate here on its susceptibility

$$\chi = N(\langle D^2 \rangle - \langle D \rangle^2), \tag{5}$$

which diverges at the phase transition temperature T_c. On finite systems, the divergence in χ is smoothened into a finite maximum $\chi_{\max}(L)$ at some pseudocritical temperature $T_{\max}(L)$. Finite-size scaling predicts the following two fundamental scaling relations (see, e.g., Refs. [28–30])

$$\chi_{\max}(L) \sim L^{\gamma/\nu}, \tag{6}$$

$$T_{\max}(L) = T_c + aL^{-1/\nu}, \tag{7}$$

which are the primary means used in this paper to obtain the critical exponents ν, γ and the critical temperature T_c, and to discuss anomalous scaling. From MC simulations at discrete temperatures in the vicinity of the phase transition, we obtain $\chi_{\max}(L)$ and $T_{\max}(L)$ by making use of standard reweighting techniques [31] and optimization algorithms. Error estimates for these quantities are obtained by "jackknifing" this procedure [30,32].

B. Wolff-like cluster update

Up to now, the application of the PT technique has proven to be quite efficient, enabling a study of the classical (and

quantum) CM on moderately large lattice sizes [9]. However, for linear system sizes of about $L \gtrsim 100$, we observe that the method runs into problems as the equilibration times in the MC simulation become visibly very long. In order to go efficiently beyond such lattice sizes, a further improved method is therefore called for.

Indeed, as we shall propose here, a rather straightforward improvement is possible with a special one-dimensional Wolff-cluster update [33]. To see this, reconsider the ordinary Wolff-construction for $O(N)$ spin models with Hamiltonian $\mathcal{H}_{O(N)} = J\Sigma_{\langle ij \rangle} \mathbf{S}_i \mathbf{S}_j$. Following Ref. [33], the operation

$$R^{\mathbf{r}}(\mathbf{S}_i) = \mathbf{S}_i - 2(\mathbf{S}_i \cdot \mathbf{r})\mathbf{r} \tag{8}$$

denotes a reflection of the $[O(N)]$ spin $\mathbf{S}_i$ along a hyperplane defined by the vector $\mathbf{r}$. Given a random $\mathbf{r}$, Wolff clusters are constructed using the bond activation probability

$$P_{ij} = 1 - \exp(\min[0, -J\beta[\mathbf{S}_i \mathbf{S}_j - \mathbf{S}_i R^{\mathbf{r}}(\mathbf{S}_j)]) \tag{9}$$

for bonds $\langle ij \rangle$. The spins in each cluster are then flipped by applying $\mathbf{S}_i \rightarrow R^{\mathbf{r}}(\mathbf{S}_i)$ which implements the (nonlocal) MC move. The principle of detailed balance is satisfied by requiring the invariance

$$H[R^{\mathbf{r}}(\mathbf{S}_i), R^{\mathbf{r}}(\mathbf{S}_j)] = H(\mathbf{S}_i, \mathbf{S}_j) \equiv H_{ij} \tag{10}$$

of the bond energy H_{ij} ($\mathcal{H} = \Sigma_{\langle ij \rangle} H_{ij}$) under reflection of the spins for each bond $\langle ij \rangle$ of the lattice. While this is true for $\mathcal{H}_{O(N)}$, it is clearly not true for the CM in general. However, we know that for the CM, the following special reflection operations $R^{\mathbf{e}_x}$ and $R^{\mathbf{e}_y}$ with

$$R^{\mathbf{e}_y}(S_i^x, S_i^y) = (-S_i^x, S_i^y), \tag{11}$$

$$R^{\mathbf{e}_x}(S_i^x, S_i^y) = (S_i^x, -S_i^y) \tag{12}$$

are symmetries on a subset of all bonds $\langle i, j \rangle$ [2,6], namely, that

$$H[R^{\mathbf{e}_y}(\mathbf{S}_i), R^{\mathbf{e}_y}(\mathbf{S}_{i+\mathbf{e}_x})] = H(\mathbf{S}_i, \mathbf{S}_{i+\mathbf{e}_x}), \tag{13}$$

$$H[R^{\mathbf{e}_x}(\mathbf{S}_i), R^{\mathbf{e}_x}(\mathbf{S}_{i+\mathbf{e}_y})] = H(\mathbf{S}_i, \mathbf{S}_{i+\mathbf{e}_y}). \tag{14}$$

Thus, we may employ $R^{\mathbf{e}_x}$ and $R^{\mathbf{e}_y}$ to construct one-dimensional clusters of spins along the x or y direction. Employing the form of the CM Hamiltonian (1) and the general relation (9), we obtain the following bond-activation probabilities:

$$P_{ii+\mathbf{e}_x} = 1 - \exp(-2J_x \beta S_i^x S_{i+\mathbf{e}_x}^x), \tag{15}$$

$$P_{ii+\mathbf{e}_y} = 1 - \exp(-2J_y \beta S_i^y S_{i+\mathbf{e}_y}^y) \tag{16}$$

for cluster growth along the x and y directions, respectively. Note that the cluster construction is really strictly one-dimensional, i.e., when we build x clusters, we do not attempt to add y bonds to the cluster which would break condition (13). Cluster construction starts as usual by picking a random start site from which cluster growth proceeds.

An obvious difference to the original Wollf algorithm is the discrete set of possible spin reflections. Thus, the cluster update alone does not satisfy ergodicity. This is not a problem as long as ordinary METROPOLIS (as well as PT updates) are performed in addition. In each MC sweep, we perform on average L cluster updates in both x and y directions as well as N local METROPOLIS updates. We have verified by detailed comparison to existing data that the new algorithm works correctly. Let us proceed directly to an evaluation of the new update. In order to examine its performance, we ran several tests on lattice sizes $L = 16, 24, 32, 48, 64$ (96 in case of the cluster update) in the ensemble Z_{PBC} at the pseudocritical temperatures $T_{\max}(L)$ (known from our previous study). In the first test, we switched off the PT update and compared the autocorrelation time τ of the energy time series which should scale at the critical point like $\tau \sim L^z$. Figure 1(a) compares the scaling of τ with and without the above cluster updates. Clearly, we find that the cluster algorithm behaves much better. Apart from the expected absolute reduction of τ, we observe a decrease of z from $z \approx 3.5$ to $z \approx 2.5$ which is apparent from the different slopes in the log-log plot. Next, we also compared the autocorrelation time τ in simulations employing the PT algorithm. Without performing a detailed scaling analysis, it is evident from Fig. 1(b) that the cluster update further improves the PT algorithm.

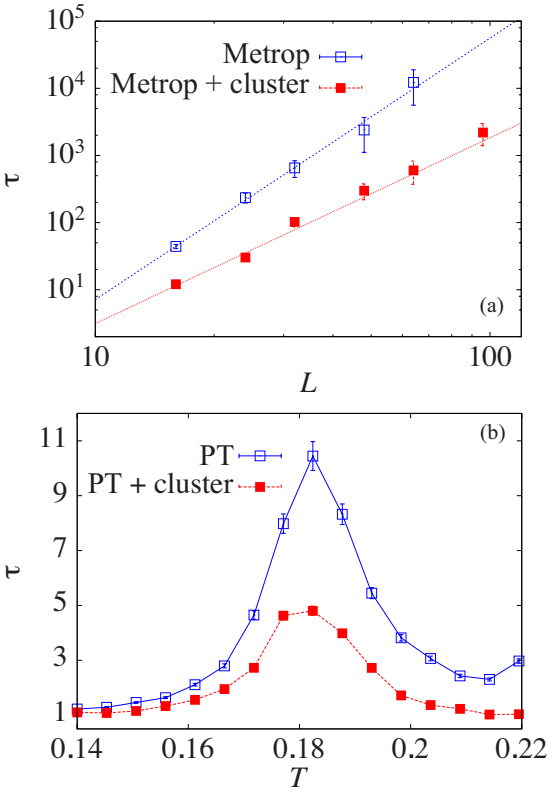

FIG. 1. (Color online) (a) Comparison of the autocorrelation time τ at the critical point using periodic boundary conditions. Comparison of $\tau(L)$ for the pure METROPOLIS and the combined METROPOLIS+cluster update. An overall improvement for τ as well as better scaling is evident for the cluster variant. (b) Comparison of τ for $L=36$ as obtained from the pure parallel tempering approach with the improved parallel tempering variant.

The methodological improvement presented here allows to study much larger system sizes than before. In the course of this study, we have performed simulations up to $L=512$.

III. CLASSICAL COMPASS MODEL: RESULTS

In this section, we are going to employ the algorithmic advances to restudy critical properties of the classical CM. Special focus is given to a more detailed comparison of ensembles Z_{FBC} and Z_{PBC}. Based on this comparison, we will thereafter propose the use of alternative boundary conditions and study their effects on FSS properties.

A. Revisiting periodic and fluctuating boundary conditions

Previous investigations of the DO transition have clearly shown that the use of ensemble Z_{FBC} is favorable over Z_{PBC} in terms of FSS properties [7,9], where the most severe "failure" of Z_{PBC} establishes itself in an unconventional behavior of the Binder parameter. Despite these observed defects, it was argued [9] that one may still employ PBC to extract the critical properties given the system sizes L are large enough. This argument was supported from extrapolations of pseudocritical temperatures $T_{\max}(L)$ which gave consistent results for both Z_{FBC} and Z_{PBC} of about $T_c=0.1464(2)$.

With the newly available cluster procedure, we will investigate this issue further to make more quantitative statements about how ensembles Z_{FBC} and Z_{PBC} converge toward another asymptotically. We have thus simulated the CM for system sizes between $L=12$ and $L=512$, pushing L a factor of 5–10 times larger than before. In comparison to Ref. [9], we have added system sizes $L=96,128,164,256,512$.

The observables described in Sec. II A were estimated using about 10^5 samples. We have taken measurements only every m MC sweep such that the final autocorrelation time was small, $\tau<10$ (m was in the range of 4–100). For a presentation of the typical temperature dependence of the order parameter and susceptibility, we refer the reader to the previous work of Ref. [9]. Here we just present the pertinent data obtained for the pseudocritical temperature $T_{\max}(L)$ and $\chi_{\max}(L)$. Figure 2 summarizes the FSS analysis for the two different ensembles considered. The partly surprising results of this comparison can be summarized as follows.

First, we observe that the FSS behavior for Z_{FBC} is fully consistent with earlier results, i.e., data obtained on larger lattices agree with the extrapolations from smaller lattice sizes. This further confirms the claim of 2D Ising universality beyond any reasonable doubt. Indeed, fits to Eq. (7) yield our estimate of the critical temperature and critical exponent as

$$T_c=0.14621(2), \quad \nu=1.00(1), \tag{17}$$

(with $\chi^2/\mathrm{d.o.f}=1.4$ where d.o.f. denotes the number of degrees of freedom) which represents an improvement of roughly 1 order of magnitude over the previous estimate. Together with the critical exponent $\gamma=1.75(1)$ obtained from analyzing the scaling of $\chi_{\max}$, this is in perfect agreement with the exactly known critical exponents for the 2D Ising model.

Second—and this is the surprising result—the scaling for Z_{PBC} reveals a more complicated or stronger *anomalous scaling* than previously thought. This is especially apparent in Fig. 2(a) where pseudocritical temperatures for $L>96$ clearly deviate systematically from the previous extrapolation [upper (blue) straight line] of Ref. [9] based on the assumption of 2D Ising scaling for $L>30$. Note that the upper (blue) line was also justified because it matched exactly with the result from Z_{FBC}. However, instead of a clear power law scaling in $1/L$, we observe a "double bend" in the FSS curve which seems to collapse onto the curve from Z_{FBC} for very large system sizes $L\geq 256$ [inset of Fig. 2(a)].

The same anomalous scaling behavior shows up in the quantity $\chi_{\max}(L)/N$ of Fig. 2(b) which shows a strong nonmonotonic behavior at a length scale of about $L\approx 120$. Thus,

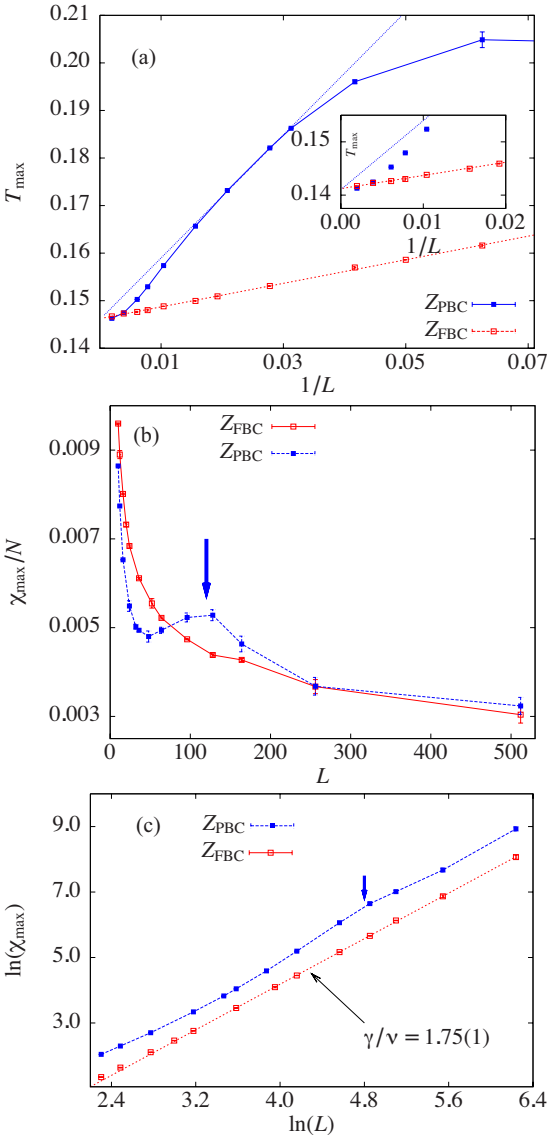

FIG. 2. (Color online) Improved finite-size data for the classical compass model with PBC and FBC. (a) Extrapolation of the pseudocritical temperatures $T_{\max}(L)$. Data for FBC follow a perfect straight line. The periodic case shows a clear bend for system sizes $L>96$ not anticipated before based on the straight line extrapolation in Ref. [9]. (b) The susceptibility maxima divided by N behave nonmonotonously and indicate a resonance phenomenon at about $L\approx 120$ (indicated by the arrow). (c) FSS of $\chi_{\max}$ in a log-log plot. For FBC, a power law is evident with $\gamma/\nu=1.75(1)$. For PBC, a power-law extrapolation is not justified and different scaling regimes are apparent.

any attempt to extract the critical exponent γ from a log-log plot as in Fig. 2(c) is doomed to fail on length scales below $L \approx 256$. The observed nonmonotonic behavior also shows up in the Binder parameter but we postpone a discussion on that to the next subsection.

As a matter of fact, it is thus totally unreliable to obtain critical exponents and the critical ordering temperature T_c from simple extrapolations in the ensemble Z_{PBC} on periodic lattices (at least for $L \lesssim 256$). The previous seemingly correct extrapolation was a matter of coincidence. Turning this observation around, one might even be tempted to argue for non-Ising behavior in the CM if one did not have access to the largest lattice sizes studied here. This situation is most unsatisfying and calls for a deeper investigation and a workaround. We will attempt precisely this in the next subsection.

B. Screw-periodic boundary conditions

The main message of the discussion so far is that PBC shows a more complex scaling behavior than previously thought with the appearance of a clear resonance effect and at least two different scaling regimes. This disqualifies the use of PBC to extract critical properties. The FBC ensemble on the other hand also has—despite its intriguing performance—a couple of drawbacks. The most important of all is that we may not easily use it in QMC because fluctuating couplings induce a minus-sign problem. Second, one may wonder whether it is safe to use them in the first place as a trustable FSS theory is not available and one is actually simulating a different model. Here, we would like to ask whether it is nevertheless possible to deal with the described problem using only slightly modified boundary conditions without going to a higher-dimensional configuration space.

It is quite obvious that the torus geometry hides or shields the true physics going on. One possibility to unveil the true properties of the CM in the thermodynamic limit is to introduce systematic deformations to the torus. In this way, we can at least see how the problem is alleviated (or made worse). Among all such deformations, one may consider a Möbius strip or so-called screw-periodic boundary conditions. Such deformations are very easy to implement on the computer and cost no extra updates. We decided to study screw-periodic boundary conditions (SBC) which are defined by

$$(x,y+1) = \begin{cases} (x,y+1) & \text{if } y < L-1 \\ ([x+S] \bmod L, 0) & \text{if } y = L-1, \end{cases}$$

$$(x+1,y) = \begin{cases} (x+1,y) & \text{if } x < L-1 \\ (0,[y+S] \bmod L) & \text{if } x = L-1, \end{cases} \tag{18}$$

where, e.g., $(x,y+1)$ denotes the nearest neighbor of site $i=(x,y)$ in y direction. The parameter S is a parameter that determines how much we deform the clean torus case. Figure 3 illustrates this concept for two cases $S=1$ and $S=2$. The cases $S=0$ and $S=L$ are obviously identical to the usual PBC. For a given lattice size, S may take only certain values in order to satisfy the overall periodicity constraint. The possible S values are given by the set of all (distinct) divisors of L. SBC are discussed in various forms in the literature, sometimes called helical boundary conditions or shift boundary conditions. Mostly, they have been employed because they have some advantages regarding implementation issues [29,34] or to complement FSS analysis [35] as they approach the thermodynamic limit with (slightly) different pseudocritical temperatures. A further useful application is the controlled formation of *tilted* domain walls in the Ising model [36]. Note that each site still has exactly four neighbors which distinguish SBC from open boundary conditions.

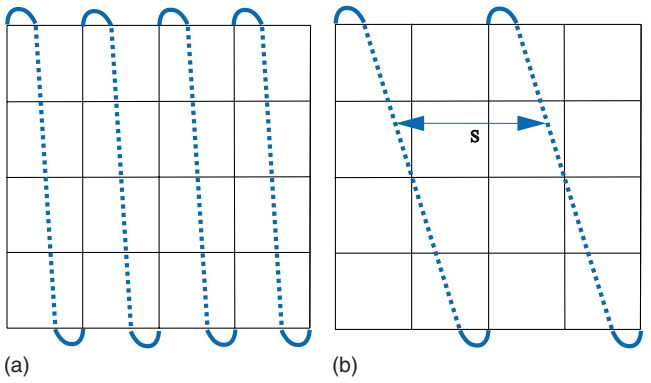

FIG. 3. (Color online) Illustration of screw-periodic boundary conditions along the y axis as defined in Eq. (18). Two examples with (a) $S=1$ and (b) $S=2$ are shown. In our simulations, the same procedure is applied to the x direction.

SBC allows one to put the lattice points into representation classes which we will call loops. A loop is the set of all points i that the screw or helix passes until it closes itself. The length of a loop is called L_l and is the number of points it contains. Each point i is obviously member in exactly two loops: one for the x and one for the y direction. Given a lattice size L and compatible screw parameter S, each loop has length $L_l = L^2/S$ and for $S=1$, all points belong to the same loop. The notation introduced here becomes relevant when discussing the symmetry properties of the CM and its ground-state degeneracies.

A simple check confirms that the usual one-dimensional spin flip operators $P_l = \Pi_x \sigma^y_{(x,l)}$ and $Q_m = \Pi_y \sigma^x_{(m,y)}$ [2,6] (which are related to operations $R^{\mathbf{e}_x}$ and $R^{\mathbf{e}_y}$ in Sec. II B) are no longer symmetries of the (quantum) Hamiltonian (1) if $S \neq 0$. However, they can be generalized to the SBC case with the following operators:

$$P_l = \prod_{j \in l} \sigma^y_j, \tag{19}$$

$$Q_m = \prod_{i \in m} \sigma^x_i, \tag{20}$$

where l and m now refer to a loop along the x or y direction. As we can control the number of independent loops via the parameter S, we can control the number of such symmetry operators and thus the degeneracy of the ground state. Indeed, it is possible to change the ground-state degeneracy from exponential growth $2^{L+1}(S=0)$ to a constant 2 $(S=1)$, an observation which may have interesting physical conse-

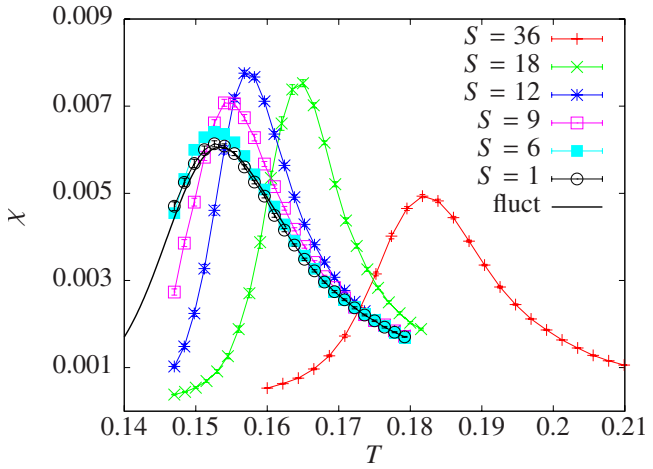

FIG. 4. (Color online) Dependency of the susceptibility $\chi(T)$ for $L=36$ on the choice of the screw parameter S. The case $S=36$ is equivalent to periodic boundary conditions. With decreasing S (or increasing the boundary loop length), a clear shift in the peak is observed with an apparent resonance at $S\approx 12$. For $S=1$, the susceptibility is (nearly) identical to the susceptibility obtained in the fluctuating bond ensemble Z_{FBC} (continuous line without symbols).

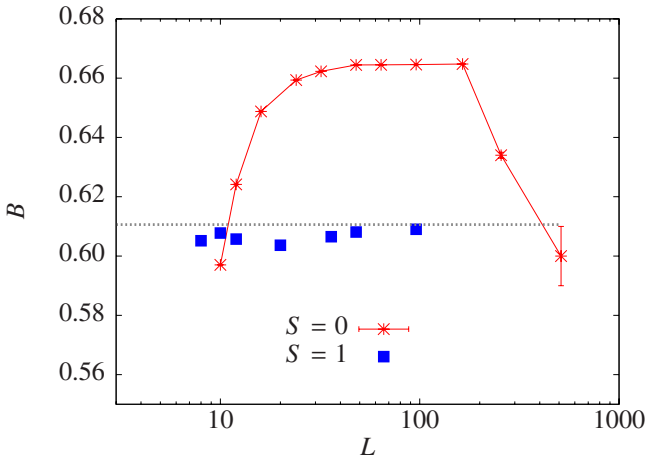

FIG. 5. (Color online) Finite-size behavior of the Binder parameter B at the critical point $T=T_c$ for periodic ($S=0$) and screw boundary conditions with $S=1$. While there is a strong anomaly for $S=0$, the case $S=1$ almost completely removes the defect and is consistent with a scale-independent value of B at the critical point. Moreover, it is consistent with the usual 2D Ising value [37,38] indicated by the horizontal line. Note that the symbol size for $S=1$ is bigger than the error bar.

quences. The thermal DO transition studied here should not be affected by this as the relevant global Z_2 symmetry is not changed.

Let us proceed to study the effect of SBC in actual MC simulations. To this end, we choose a system size $L=36$ which allows us to study quite a large number of screw parameters $S=0,1,2,3,4,6,9,12,18$. In each case, we measured the order parameter D and its susceptibility χ for a couple of temperatures close to the phase transition. Figure 4 depicts the drastic effect of SBC on the susceptibility χ. Starting from the periodic case $S=0$ (or $S=36$), we observe that χ moves massively toward the curve from Z_{FBC} for decreasing $S>0$ or increasing L_l. The case $S=1$ gives an almost identical result to that obtained with fluctuating couplings in the Z_{FBC} ensemble. Second, it is apparent that there is a resonance at some length scale determined by $S\approx 12$ at which the fluctuations in the system are strongest.

The above picture thus suggests that $S=1$ resolves the FSS problems observed in the CM for the susceptibility almost completely. Furthermore, it gives a hint at the order of the disturbing length scale ($L_l\approx 36^2/12\approx 110$) which is present and which prohibits the extraction of correct critical data. Any solution that restores good FSS properties should also repair the behavior of the Binder parameter

$$B = 1 - \frac{1}{3}\frac{\langle D^4\rangle}{\langle D^2\rangle^2}, \tag{21}$$

whose normally used power is due to a scale invariance at the critical point with only leading-order corrections. Thus, if SBCs really solve the problem, they should also remove the very unconventional behavior in the Binder parameter which was observed with PBC in Ref. [9]. Figure 5 shows a comparison of the finite-size behavior of B for the cases $S=0$ (periodic) and $S=1$ performed close to the critical point given in Eq. (17). The periodic case shows the expected non-monotonous behavior (with a possible restoration for $L>256$). The $S=1$ screw restores the expected scaling behavior—up to a small bump for $L<12$—completely, i.e., it is almost a constant for various system sizes and agrees rather well with the known value of $B\approx 0.61$ [37,38] for the 2D Ising model (constant line in Fig. 5). Note, however, that the agreement is not expected to be perfect as boundary conditions can have (a small) influence on the (only weakly universal) critical value of B [39]. For an analysis of the Binder parameter for FBC, we refer the reader to Ref. [9].

This brings us into the position to claim that SBCs are a very efficient tool to study critical properties of the CM. Before we apply these to the quantum CM, let us try to shed some light onto the origin of anomalous scaling (with PBC).

C. Origin of anomalous scaling: One-dimensional spin order

It is evident from the MC analysis in Secs. III A and III B that there is a second length scale in the CM which influences fluctuations and which can be overcome by SBC. Let us now turn to a discussion of possible reasons for this as a more fundamental understanding of this phenomenon is clearly desirable.

We know that the low-T (directionally ordered phase) of the CM is essentially one-dimensional where the spins along each row or column are essentially decoupled. These spins thus form a one-dimensional (1D) spin chain. Using this picture, a plausible explanation for the failure of FSS was actually suggested in Ref. [7] where it is argued that the *magnetic* spin-spin correlation length ξ_{1D} along each chain exceeds the linear system size L at low temperatures. If this were the case, all spins would align themselves along each chain although a directionally ordered state can survive even with domain walls in spin space. Such total magnetic ordering

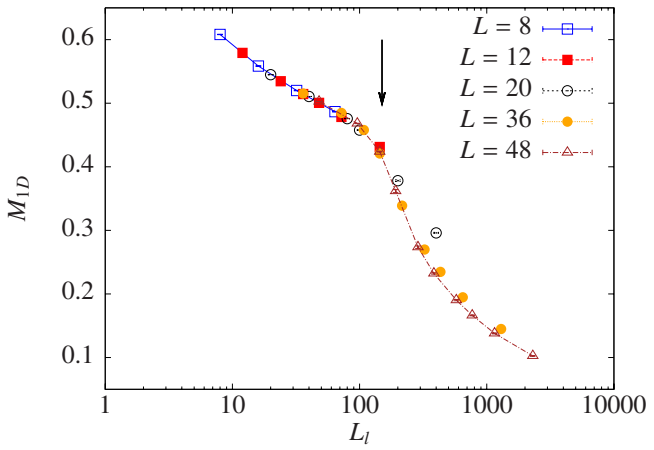

FIG. 6. (Color online) Expectation values for one-dimensional magnetization for several lattice sizes and choices of the screw displacement S at the critical temperature T_c. The x axis is the loop length $L_l=L^2/S$. Data from different lattice sizes collapse onto one curve (for $L_l \lesssim 100$). A clear crossover from a region with finite magnetization to a disordered spin state is observed on a length scale $L_l \approx 100$ (indicated by the arrow). This length scale corresponds to those where anomalies are seen in the FSS analysis.

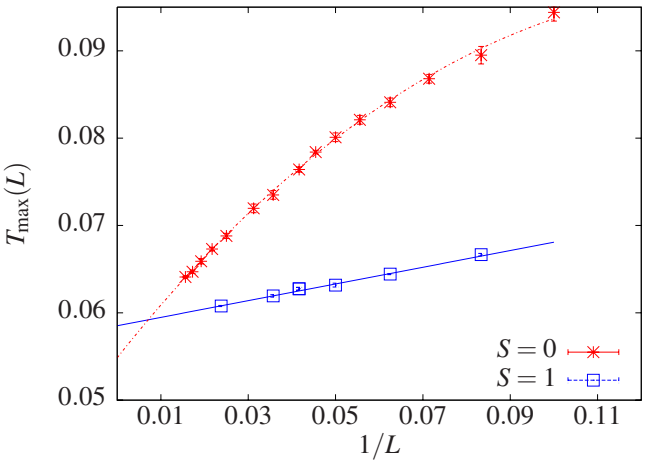

FIG. 7. (Color online) FSS plot of the pseudocritical temperatures for the quantum CM from the susceptibility comparing periodic ($S=0$) and screw-periodic boundary conditions ($S=1$). The latter clearly leads to a considerable improvement. The line is a fit using a power law correction in $1/L$. The dashed extrapolation of data from periodic boundary conditions [9] underestimates the critical temperature as expected from the discussion in Sec. III A.

tendency could influence the fluctuations of the true order parameter, making it more robust against thermal fluctuations and spoiling its FSS properties.

To test this hypothesis, let us write down an order parameter for such one-dimensional magnetic ordering tendency M_{1D} as

$$M_{1D}^{x(y)} = \frac{1}{N_L} \sum_{x(y)\ \text{loops},\ l} \frac{1}{L_l} \left| \sum_{i \in l} S_i^{x(y)} \right|, \tag{22}$$

$$M_{1D} = \frac{1}{2}(M_{1D}^x + M_{1D}^y). \tag{23}$$

Here, N_L denotes the number of boundary loops (as introduced above) and L_l the length (number of sites) of loop l, i.e., we already take care for the general screw-periodic case. The quantity M_{1D} probes whether all spins along each chain (or loop) like to align themselves.

To test whether such possible (long-range) ordering of the spins exists on top of directional order, we perform a couple of MC runs at the critical temperature T_c obtained in Eq. (17) for lattice sizes $L=8,12,20,36,48$. In each case, we simulate all possible screw parameters S. In Fig. 6, we plot the expectation values of M_{1D} vs the screw loop length $L_l=L^2/S$. Remarkably, the data from different system sizes collapse onto the same curve for $L_l \lesssim 100$ where a finite expectation value for M_{1D} is evident. This magnetic suborder does not persist in the thermodynamic limit as for $L_l \gtrsim 100$ it suddenly approaches 0. We conclude that there is a strong tendency for the spins to align themselves which is enforced by PBC. Application of SBC can overcome this problem because it exceeds the typical length scale along each loop. The same is true for FBC by artificially introducing kinks in the spin configurations, which is the basic reason why they do not show anomalies such as those in Fig. 2(b).

The length scale L_c at which the sudden decrease in M_{1D} appears coincides precisely with the nonmonoticities observed in the scaling of T_{max} and χ_{max} of Fig. 2. The resonance effect in Fig. 4 can be explained because at $L_l=L_c$, we have strong fluctuations in M_{1D} in addition to the normal fluctuations in the directional-order parameter D.

These results essentially confirm the picture of Ref. [7] and quantify precisely the length scale involved. The quite large magnetic correlation length can be understood by recalling the exponential divergence of the magnetic correlation length at low temperatures in the 1D Ising model.

IV. RESULTS FOR THE QUANTUM CASE

We have now developed everything to proceed to the main objective of this paper which is to improve the estimate of the critical ordering temperature T_c for the DO transition in the presence of quantum fluctuations. Due to the results of Sec. III A, it is probable that the previous result $T_c=0.055(1)$ in Ref. [9] is slightly off the true critical temperature due to the presence of the second length scale.

We expect that SBC rectify and improve this value. Therefore, new QMC simulations in the stochastic series expansion (SSE) framework using directed loops [40,41] and PT updates were performed implementing $S=1$ SBC. Otherwise, our approach rests on that presented in Ref. [9] where concrete implementation issues are discussed. A couple of simulations for lattice sizes $L=10,12,16,20,24,28,32,42$ were performed and approximately 100 000 statistically independent samples of the order parameter D were taken in each case. The pseudocritical temperatures $T_{max}(L)$ were obtained from the peak in the variance of D utilizing the quantum generalization of the multihistogram reweighting idea [42]. Figure 7 shows the pseudocritical temperatures obtained and compares them to the old data utilizing PBC. As

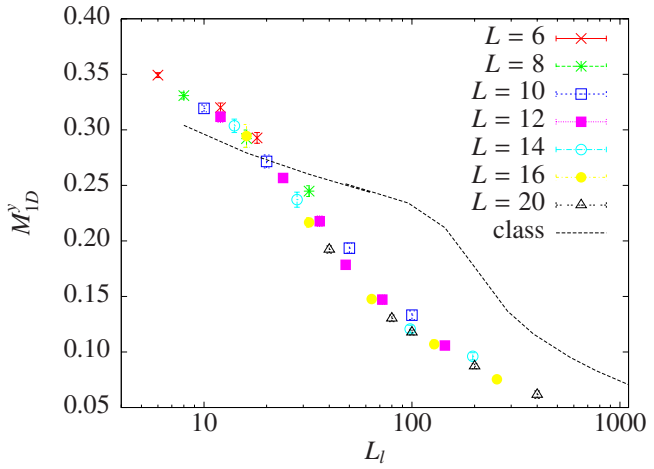

FIG. 8. (Color online) Analysis of the one-dimensional magnetization M^y_{1D} for the quantum CM. The result from the classical case is indicated by the line taken from Fig. 6 (and divided by a factor 2). The magnetic length scale is clearly much larger in the classical case.

expected, an evidently improved FSS behavior is observed for the screw-periodic case. This is apparent from the absolute move of $T_{\max}$ toward the true critical temperature for small L *and* the much better power-law scaling in terms of $1/L$. Indeed, the SBC data are fully consistent with $\nu=1$ and a straight line fit to

$$T_{\max}(L) = T_c + aL^{-1} \tag{24}$$

yields our new estimate for the critical temperature as

$$T_c = 0.0585(3), \tag{25}$$

with $\chi^2/\text{d.o.f}=1.5$ using all lattice sizes studied. Even using only the of smallest systems $L=12$ to $L=20$, the extrapolation yields a consistent value of $T_c=0.058(1)$, a property which is of most practical relevance for studies aiming at numerically verifying more qualitative effects (see, e.g., Ref. [8]). Leaving ν as a free fit parameter as in Eq. (7), we obtain $T_c=0.0586(8)$ and $\nu=0.97(15)$ which is consistent with 2D Ising behavior. Hence, although we have performed much less simulations *and* on smaller system sizes, we have obtained a much better and improved result just by an adequate choice of the boundary conditions. The present result does not agree within error bars with the previous estimate $T_c=0.055(1)$ because of the anomalous behavior which was not accounted for in the ordinary Ising extrapolation (dashed line in Fig. 7) with a $L^{-\omega}$ correction on periodic lattices. However, it appears that the effect of the magnetic length scale is not as severe as in the classical case. This could be expected due to the presence of quantum fluctuations. On the other hand, the temperature regime is lower which could in principle even stabilize the unwanted order. In order to get an approximate estimate for the length scale involved, we have finally analyzed the one-dimensional magnetization also for the quantum case, where we restrict ourselves to measure M^y_{1D} (which corresponds to the quantization direction) along y loops. Figure 8 shows the SSE estimates for M^y_{1D} for various system sizes and screw parameters at $T=0.07$ (chosen for convenience because it is close to T_c and still in the region where PBC show unusual behavior). It verifies that quantum fluctuations reduce the overall value of M^y_{1D} and that they lead to a clear diminution of pseudomagnetic order at a scale corresponding to roughly $L\approx 50$ which is apparently smaller than in the classical case (line in Fig. 8). Moreover, we also arrive at this conclusion by studying the behavior of the susceptibility in dependence on S (similar to that in Fig. 4) and observe that the resonance is shifted to a smaller length scale in accordance with the findings just described. However, even such a moderate scale can still be a formidable challenge to overcome for QMC without SBC.

TABLE I. Previous and current estimates of the critical temperature of the DO transition exemplifying the (previous) difficulty of its extraction.

T_c	System sizes	Boundary cond.	Method	Ref.
0.075(2)	10–20	Periodic	Trotter QMC	[8]
0.055(1)	10–96	Periodic	SSE+PT	[9]
0.058(1)	12–20	Screw	SSE+PT	This work
0.0585(3)	12–42	Screw	SSE+PT	This work

In summary, the estimate of T_c for the quantum CM has seen several steps of adjustments on a relatively short time scale as summarized in Table I. The result of this section provides an improved benchmark estimate which should be useful for future studies.

V. SUMMARY AND CONCLUSIONS

Summarizing, we have revisited the directional-ordering transition in the classical and quantum compass models employing two types of methodological advances. In the classical case, we were able to formulate a special one-dimensional cluster update which in combination with METROPOLIS and PT methods allowed to investigate much larger system sizes than before. The following detailed comparison between the classical CM with periodic boundary conditions and a fluctuating bond ensemble showed that periodic boundary conditions scale much worse than known so far. Instead of the usual power law, anomalous scaling becomes evident with a resonance and nonmonotonic behavior in the susceptibility and the Binder parameter at length scale of about $L\approx 100-200$. In any typical MC simulation, one would therefore not be able to predict critical properties correctly when the simulation is done with periodic boundary conditions. This resonance is argued to be due to a magnetic correlation length which prohibits the formation of domain walls at finite temperature on small clusters. To counteract this problem, we have proposed to employ screw-periodic boundary conditions. We have shown that they are able to remove scaling anomalies in the classical case almost completely.

This concept then proved to be a key step for simulations of the quantum compass model where we were able to obtain a more accurate estimate of the critical DO temperature

based only on the change in boundary conditions. On the physical side, we have seen that the CM represents a formidable challenge despite its simplicity—even for well-settled numerical approaches. The right choice of boundary conditions or topology is more essential for numerical studies of the CM than for many other models.

Technically, it is clear that screw-periodic boundary conditions should be used in future studies of various other aspects in the quantum compass model. Moreover, we regard SBC as a well-suited and general method which deserves more attention even in studies of other systems. Via the screw parameter S, one may be able to tune or minimize corrections to scaling. We are currently applying them to further studies of the quantum phase transition in 2D dimerized Heisenberg models (see, e.g., Ref. [43]).

ACKNOWLEDGMENTS

S.W. thanks the MPIPKS for support through its visitors program. The numerical work of this paper was performed on the GRAWP cluster at the Institute for Theoretical Physics of the University of Leipzig, on the CALLISTO cluster at EPFL, and on the JUROPA capability computer at NIC/JSC, Forschungszentrum Jülich under Grant No. HLZ12.

[1] K. Kugel and D. Khomskii, Sov. Phys. Usp. **25**, 231 (1982).
[2] B. Douçot, M. V. Feigel'man, L. B. Ioffe, and A. S. Ioselevich, Phys. Rev. B **71**, 024505 (2005).
[3] P. Milman, W. Maineult, S. Guibal, L. Guidoni, B. Douçot, L. Ioffe, and T. Coudreau, Phys. Rev. Lett. **99**, 020503 (2007).
[4] S. Gladchenko, D. Olaya, E. Dupont-Ferrier, B. Douçot, L. Ioffe, and M. Gershenson, Nat. Phys. **5**, 48 (2009).
[5] G. Jackeli and G. Khaliullin, Phys. Rev. Lett. **102**, 017205 (2009).
[6] J. Dorier, F. Becca, and F. Mila, Phys. Rev. B **72**, 024448 (2005).
[7] A. Mishra, M. Ma, F.-C. Zhang, S. Guertler, L.-H. Tang, and S. Wan, Phys. Rev. Lett. **93**, 207201 (2004).
[8] T. Tanaka and S. Ishihara, Phys. Rev. Lett. **98**, 256402 (2007).
[9] S. Wenzel and W. Janke, Phys. Rev. B **78**, 064402 (2008).
[10] W. Brzezicki, J. Dziarmaga, and A. M. Oleś, Phys. Rev. B **75**, 134415 (2007).
[11] E. Eriksson and H. Johannesson, Phys. Rev. B **79**, 224424 (2009).
[12] K.-W. Sun, Y.-Y. Zhang, and Q.-H. Chen, Phys. Rev. B **79**, 104429 (2009).
[13] V. W. Scarola, K. B. Whaley, and M. Troyer, Phys. Rev. B **79**, 085113 (2009).
[14] S. Wenzel and W. Janke, Phys. Rev. B **80**, 054403 (2009).
[15] C. Xu and J. E. Moore, Phys. Rev. Lett. **93**, 047003 (2004).
[16] Z. Nussinov and E. Fradkin, Phys. Rev. B **71**, 195120 (2005).
[17] C. D. Batista and Z. Nussinov, Phys. Rev. B **72**, 045137 (2005).
[18] J. Vidal, R. Thomale, K. P. Schmidt, and S. Dusuel, Phys. Rev. B **80**, 081104(R) (2009).
[19] A. Y. Kitaev, Ann. Phys. **303**, 2 (2003).
[20] H.-D. Chen, C. Fang, J. Hu, and H. Yao, Phys. Rev. B **75**, 144401 (2007).
[21] R. Orús, A. C. Doherty, and G. Vidal, Phys. Rev. Lett. **102**, 077203 (2009).
[22] J. Jordan, R. Orús, G. Vidal, F. Verstraete, and J. I. Cirac, Phys. Rev. Lett. **101**, 250602 (2008).
[23] L. Cincio, J. Dziarmaga, and A. M. Oleś, e-print arXiv:1001.5457.
[24] G. Vidal, Phys. Rev. Lett. **101**, 110501 (2008).
[25] C. Geyer and E. Thompson, J. Am. Stat. Assoc. **90**, 909 (1995).
[26] K. Hukushima and K. Nemoto, J. Phys. Soc. Jpn. **65**, 1604 (1996).
[27] E. Bittner, A. Nußbaumer, and W. Janke, Phys. Rev. Lett. **101**, 130603 (2008).
[28] A. Pelissetto and E. Vicari, Phys. Rep. **368**, 549 (2002).
[29] D. P. Landau and K. Binder, *A Guide to Monte Carlo Simulations in Statistical Physics*, 1st ed. (Cambridge University Press, Cambridge, England, 2000).
[30] W. Janke, Lect. Notes Phys. **739**, 79 (2008).
[31] A. M. Ferrenberg and R. H. Swendsen, Phys. Rev. Lett. **63**, 1195 (1989).
[32] B. Efron, *The Jackknife, the Bootstrap, and other Resampling Plans* (Society for Industriell and Applied Mathematics, Philadelphia, 1982).
[33] U. Wolff, Phys. Rev. Lett. **62**, 361 (1989).
[34] M. E. J. Newman and G. T. Barkema, *Monte Carlo Methods in Statistical Physics*, 1st ed. (Oxford University Press, Oxford, 1999).
[35] H. Kitatani and T. Oguchi, J. Phys. Soc. Jpn. **61**, 1598 (1992).
[36] E. Bittner, A. Nußbaumer, and W. Janke, Nucl. Phys. B **820**, 694 (2009).
[37] G. Kamieniarz and H. Blöte, J. Phys. A **26**, 201 (1993).
[38] J. Salas and A. D. Sokal, J. Stat. Phys. **98**, 551 (2000).
[39] W. Selke, Eur. Phys. J. B **51**, 223 (2006).
[40] A. W. Sandvik, Phys. Rev. B **59**, R14157 (1999).
[41] O. F. Syljuåsen and A. W. Sandvik, Phys. Rev. E **66**, 046701 (2002).
[42] M. Troyer, S. Wessel, and F. Alet, Braz. J. Phys. **34**, 377 (2004).
[43] S. Wenzel, L. Bogacz, and W. Janke, Phys. Rev. Lett. **101**, 127202 (2008).
[44] Or one arbitrary bond on each row and column of the lattice.